EGE

EARTH OBSERVATION AND GEOMATICS ENGINEERING

Study on the radioactive pollution in urban features using knowledge-based fuzzy classification of VHR satellite imagery

Alireza Arabsaeedi[1], Abbass Malian[1]*, Mahdi Arabi[1]

[1] Department of Geomatics Engineering, Shahid Rajaee Teacher Training University, Tehran, Iran

ABSTRACT

Safety is of primary principles of living in human communities. Preparation and provision of necessary considerations for encountering hazards are main targets of the crisis management. Nuclear risks are one of hazards threatening in the human life. Since radioactive contaminants sustain for years after the incident, investigation into nuclear hazards and its damage on living environment and urban features is so vital. This study essentially aims at evaluating the risk of radioactive contaminants to urban land uses. Due to high resolution satellite images, remote sensing technology has been considered as an advanced technology to generate information covering urban areas. Information on land cover is one of the most important tools of management during crisis. Land cover maps can be prepared through techniques for high resolution satellite image processing and extracting urban features. In this study, the fuzzy object-oriented method is applied to classify such phenomena. In the proposed method, a fuzzy rule-based strategy and hierarchical model are employed to overcome noise between classes. Fuzzy rule-based classification method is used as well as optimization and improving features of multi-scale analysis. Considering blocks of WorldView2 sensor, 91% of object detection is implemented with an average accuracy. When classification image of urban features is produced, the risk of radioactive contaminants to each recognized object is determined based on EDEM model.

1. Introduction

Detection and classification of urban features is concerned by remote sensing researchers in order to establish, implement and update spatial databases. Using satellite image processing techniques, remote sensing science as an advanced technology plays a key role in recognizing objects. According to quick progresses in various scopes such as improvement in resolution and satellite image processing techniques, it is necessary to assess different methods for detection of features in order to research into particular purposes. Risk assessment of each urban phenomenon through disasters is one of principal targets of national security and sustainable development. Sensitive national infrastructures and features include nuclear power plants and utilities. Nuclear power plants cause hazards despite their advantages in national industry. So in addition to take advantage of this advanced technology and science, security and control of the hazards must be explored. As an accurate practical science, remote sensing can be so beneficial to recognize sensitive risky points and provide geospatial information for modeling a phenomenon. Therefore, it is possible to monitor, analyze and assess previous nuclear disasters comprehensively and precisely using capabilities such as accessibility, repeatability and integrated remote sensing datasets. Objects and properties of complicated, concentrated urban landscapes should be classified separately. Remote sensing technology has presented new capabilities by high resolution satellite images. High resolution images make it possible to extract more data on land features. But such images make problems in detection

of objects with similar spectral and textural properties. Object-oriented systems are able to create different levels of segmentation by various parameters. Many researchers have applied object-oriented analyses to classify urban land covers using high resolution satellite images. In those researches, texture information and reflectance properties of objects was used. These approaches were usually suitable for semi-residential areas and a limited number of classes were detected (Gamanya et al., 2009; Liu et al., 2006; Steinnocher et al., 2005). In another study, building classification was done using support vector machines through object-based and pixel-based analysis and the data was applied due to dense vegetation of the area and laser pulse penetration into tree branches (Jordi, 2007). Zhou et al (2009) proposed an object-based approach to analyze and detect layout of urban landscapes on parcel level using high resolution aerial images and laser data. In their study, an additional geospatial database including border properties of segments and building footprints were used to facilitate the segmentation and provide more precise classification. The advantage of the study was benefiting from laser data capabilities to distinguish class of trees from shrubs and using a secondary database to distinguish between roads and sidewalks. Object-based classification of VHR images represents a viable alternative to the traditional pixel-based approach minimizing the intra-class spectral variation using objects (Jinmei & Guoyu, 2011; Liu and Xi, 2010). Numerous studies have addressed comparative analysis between the pixel-based and the object-based classification. Besides many advantages, the main drawback of object-based classification is the dependency of the final accuracy on the quality of the segmentation results (Whiteside et al., 2011; Ouyang et al., 2011; Cheng and Han, 2016). Therefore, achieving a desirable degree of accuracy for segmentation and/or classification using objects require a large amount of time and parameterization of algorithms (Achanta et al., 2012). In the last decades, the object-based image analysis (OBIA) has emerged as a sub-discipline of GIScience devoted to analysis and processing of very high resolution (VHR) satellite imagery (Sowmya & Sheela, 2011). Image segmentation aims to partition relatively homogeneous image objects, non-overlapped and spatially adjacent. There are many approaches and methods for classification and the most commonly used approaches involve statistical modelling like maximum likelihood classification, neural networks based approaches and support vector machines. Image classification is one of the most commonly used methods to extract land cover information from remote sensing images and has been widely studied over the past three decades (Wilkinson, 2005). In many applications of spatial imagery, there is often a discrepancy between automated analysis methods and direct interpretation by a specialist. In this context, an important challenge is to integrate expertise in Satellite Image Time Series (SITS) analysis to improve the reliability and precision of the results. An expert knowledge-based SITS analysis method for land use monitoring is presented by (Rejichi et al., 2015). In this method, as a first step, a multi-temporal knowledge base is created to describe the scene, utilizing expert conceptual information. Then, the temporal evolution of each region in SITS is modeled using graph theory. Finally, according to a user scenario, the most similar temporal evolution of the region is identified using the marginalized graph kernel (MGK) similarity criterion.

Traditionally, image classification is performed by a maximum likelihood, or Bayesian classifier, which assigns the most likely class to the observed data, and is known to be optimal if the assumptions about the probability density functions are correct. In classical cluster analysis each pixel must be assigned to exactly one cluster. Fuzzy cluster analysis relaxes this requirement by allowing gradual memberships, thus offering the opportunity to deal with data that belong to more than one cluster at the same time. Various image classification techniques, supervised approaches in particular, have been developed with many successful case studies. Recently developed classification techniques include support vector machines (SVMs), random forests, and sparse representation-based methods (Ham et al., 2005). Although these supervised classifiers exhibit a very promising performance in terms of classification accuracy, they mainly focus on multiclass classification. Multiclass classifiers require all classes that occur in a study area to be exhaustively labelled (Sanchez, 2011). Moreover, the goal in many cases is to optimize the classification accuracy for all land cover classes rather than for a specific class or few classes of interest (Sanchez et al., 2007). Fuzzy analysis is applied in different areas such as data analysis, pattern recognition and image segmentation. Introducing partial membership of pixels, mixed pixels could be identified and more accurate classification results could be achieved. Classification of images is a significant step in pattern recognition and digital image processing. It is applied in various domains for authentication, identification, defense, medical diagnosis and so on. The feature extraction is an important step in image processing which decides the quality of the model to be built for image classification. With the abundant increase in data now-a-days, the traditional feature extraction algorithms are finding difficulty in coping up with extracting quality features in finite time. Also the learning models developed from the extracted features are not so easily interpretable by the humans. So, considering the above mentioned arguments, a novel image classification framework has been proposed (Ravi C., 2020). The framework employs a pre-trained convolution neural network for feature extraction. Brain Storm Optimization algorithm is designed to learn the classification rules from

the extracted features. Fuzzy rule-based classifier is used for classification. The results demonstrate that the proposed framework outperforms the traditional feature extraction based classification techniques by achieving better accuracy of classification.

Fuzzy segmentation for object-based image classification was adopted in (Lizarazo & Elsner, 2009). They used a fuzzy classification method on a segmented image to classify large scale areas such as mining fields and transit sites. In (Benz et al., 2004), Object-Oriented fuzzy analysis of remote sensing data for GIS-ready information was used. In (Saberi & He, 2013) and (Shackelford and Davis, 2003), methods for hierarchical image classification using fuzzy logic were also presented. As can be seen, fuzzy logic is quite popular in satellite image analysis. Considering the uncertainties in image pixels/segments, a fuzzy inference system can be of great help in image classification. However, existing literature still suffers from the lack of the literature with a step-by-step image classification method based on fuzzy logic. A fuzzy logic approach allows objects to be member in more than one class, reflecting the inherent uncertainty of semantically derived class categories. Fuzzy logic membership functions can be used to simulate the distributions of class values for spectral, spatial, textural and contextual object parameters. Using this property of fuzzy logic membership functions, this study proposes a method for identifying descriptive spectral, spatial, textural or contextual attributes of roof and other non-roof impervious surface objects from the distribution of parameter values in these two classes (Bardossy & Samaniego, 2002).

In this study, a fuzzy inference system is used for image classification in order to detect urban features such as buildings, roads, and etc. The focus is on establishing fuzzy membership functions for object extraction. Typically, the main concern in high resolution satellite image classification is to differentiate objects like vegetation, roads, buildings,

etc., especially in urban environments (Salehi et al., 2012). Vegetation extraction methods are probably among the most straightforward object recognition techniques in remote sensing. The Near Infrared (NIR) band plays a crucial role in this field (Jabari & Zhang, 2013; Shani, 2006). Different fuzzy supervised and unsupervised methodologies are available for the classification (Gabriela, 2007; James & Ehrlich, 1984). Application of fuzzy in supervised classification and unsupervised classification and analyzing their performance was the main objective of this paper.

According to ambiguity of urban features, laser-driven data are recommended as a suitable method for more accurate classification but they are not properly practical because of the difficult accessibility in most areas and the high cost. Considering a segmentation level, image objects were produced in most of previous studies and classification was followed on that level. There was not an optimal scale for all features in such procedure. In this study, three segmentation levels are considered in regard to the features. Satellite data are the best and most efficient information resource to monitor territorial changes. Remote sensing plays a leading role in evaluation of changes and geospatial analyses after disasters. Nuclear disasters have been already one of the most important incidents with irreversible consequences. Aimed at investigating impacts of an assumed disaster in atomic utilities of Metsamor Nuclear Power Plant in Armenia, researchers at Istanbul Technical University simulated and calculated propagation velocity of radioactive materials in case of incident (Kindap, 2008). This power plant is one of the most dangerous nuclear power plants around the world located on seismic belt. Dangerous nuclear consequences of this power plant can be roughly estimated in comparison to impacts of reactor explosion in Chernobyl accident (Figure 1). Given climatic conditions of the area such as wind velocity and direction and rainfalls, the power plant poses a serious threat to its adjacent countries.
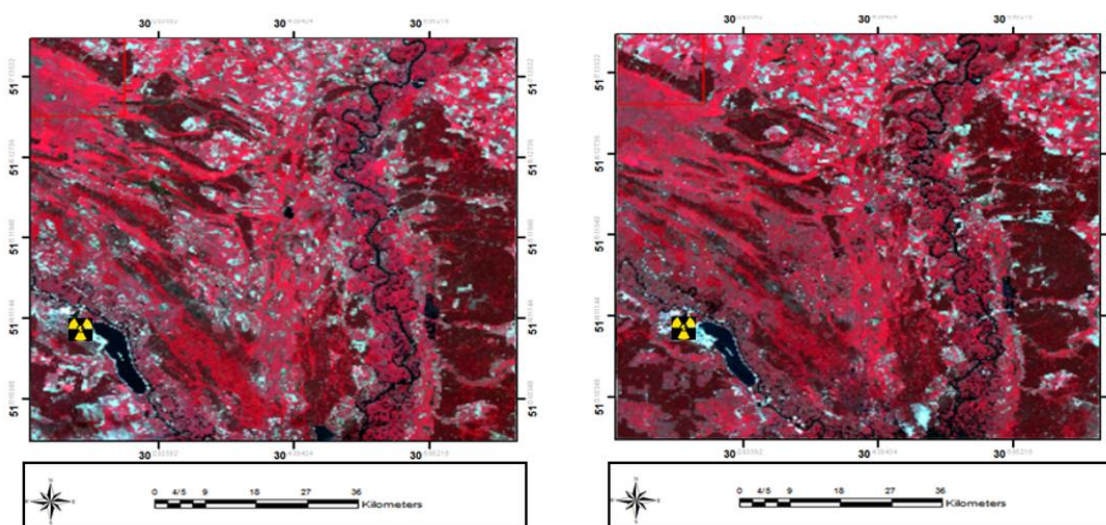

Figure 1. Satellite image of Landsat 5 showing the Chernobyl area.
Right: 1985 (Before), Left: 1987 (After)

Risk analysis can be analyzed by assessing three major components related to a specific event at a specific location (Pearce, 2000; Ramcap, 2009) – the probability of an event with a certain magnitude (hazard); the amount of potential damage measured due to a certain risk source that are exposed to the event with a certain magnitude (vulnerability); and, the costs relating to these elements (risk). In engineering fields, risk is the expected loss as a result of potentially damaging phenomena within a given time period and within a given area (Socolow et al., 1994). Hazard is defined as a potentially damaging physical event, phenomenon or human activity that may cause the loss of life or injury, property damage, social and economic disruption or environmental degradation (Douglas, 2007). This event has a probability of occurrence within a specified period of time and within a given area, and has a given intensity (Van Westen et al., 2002). To evaluate areas vulnerable to hazards, methodologies that involve the use of satellite imagery have been proposed in the recent decade usually analyze land cover maps developed through the classification of satellite images with auxiliary information such as topography, geology and geomorphology data. A mathematical expression for risk in terms of hazards and vulnerabilities can be represented according to Eq. (1):

$$Risk = Vulnerability \times Hazard \qquad (1)$$

The aim of a hazard assessment is to make a zonation of a part of the Earth's surface with respect to different types, severities, and frequencies of hazardous processes.

2. Materials and Data

The data used in this study is provided by WV2 satellite image in the north of Tehran with a concentrated urban context. According to the metadata, this image was captured on September 10th, 2014 covering 51°24´06" to 51°25´18" easting and 35°46´44" to 35°47´43" northing geographical coordinates. Image of the area is illustrated in Figure 2. As demonstrated, the area has a complex urban layout with dens features. Most of buildings have flat roofs and some sloping roofs are also observed and many buildings are hidden under trees and vegetation. The roads have asphalt surface with a spectral behaviour like building roofs. Class of buildings is more heterogeneous than roads. The images are overlaid to employ geospatial capability of grey-scale band image and spectral capability of multispectral images simultaneously on the same picture. In the current research, Gram-Schmidt transformation has been successfully applied in order to improve resolution of multi-spectral imagery. This transform has three major advantages comparing to other techniques:

1- There is no limitation on the number of simultaneously processed bands

2- This transformation can maintain low-resolution multi-spectral image characteristics in the result of fusion of the image with high-resolution panchromatic data.

This method is more robust to spatial misalignment of the bands and slight variations of input data than most other pan-sharpening methods because all transform coefficients are computed in the low MS resolution (Maurer, 2013).
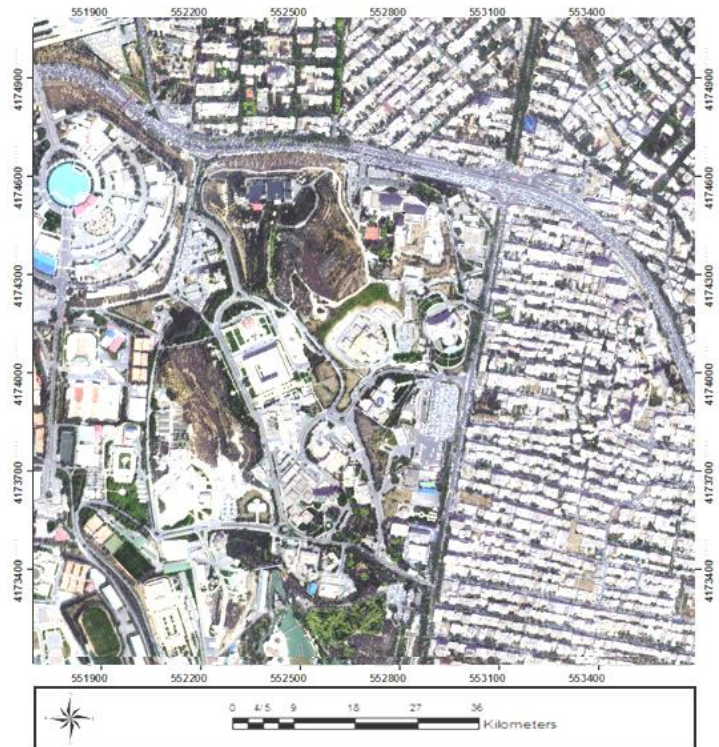

Figure 2. Satellite image WV2 showing the complexity and density of the study area in North of Tehran

3. Methodology

The proposed process employed in this research is illustrated in Figure 3.

Image classification is a robust useful approach to get thematic information from remotely sensed images. One of primary objectives of remote sensing is to detect and recognize land features. Satellite image classification can be the most important part of interpretation of satellite data. The visual procedure is accomplished in accordance with human eye ability without application of mathematical and statistical relationships based on interpretation factors such as colour, shape, texture, and image size. But numerical classification of satellite images done by computers is based on assessment of spectral value of visual components, relations between territorial features and spectral bands used in remote sensing and mathematical and statistical relationships. Numerical classification of satellite data refers to detection of similar spectral sets and rating images as classes with statistically inseparable spectrums of the same

84

spectral value. An information classification results in spectral rating and each class on new image represents features of the same value and specific domain. In fact, data classification is based on a comparison between spectral value of image pixels and introduced samples as interpreters or clusters of an unsupervised classification. The study aims to introduce and implement a method to extract land cover information using an object-based approach.
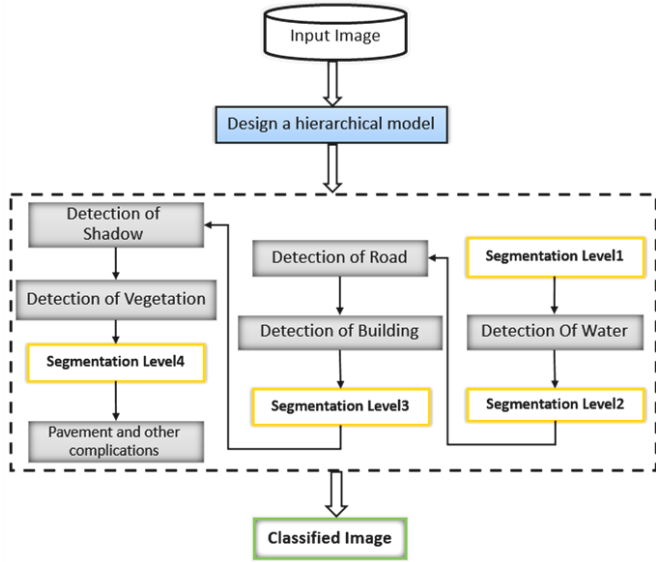

Figure 3. The proposed process for detection and classification of image object categories

3.1. Image Segmentation

Segmentation of an image is one of the most important steps of object-based analyses. Multi-resolution segmentation is applied in this study. In object-based

methods, a set of homogeneous pixels known as image objects are produced through segmentation step. Following parameters are defined to carry out segmentation procedure:

- Scale (S)
- Weight of spectral heterogeneity (W_{color})
- Weight of shape heterogeneity (W_{shape})
- Weight of smoothness (W_{smooth})
- Density (W_{compt})

Amount of scale parameter does not depend on pixel dimensions and has an unlimited domain. Shape parameter ranges between 0 and 1; as its value gets closer to 0, object detection becomes less dependent on shape and spectral distinction increases. As scale parameter changes, adjacent pixels continue to merge until relative standard deviation of final merged objects becomes less than the scale. Density parameter determines structural regularity so that as it gets closer to 1, objects become more regular structurally; of course, it causes ambiguity in distinction between linear and non-linear objects.

Correct amounts of the above parameters vary with objective of the problem so that proper value of each parameter may be obtained by trial and error. Smoothness parameter refers to similarity of the image object to its natural form. Spectral and geometrical layers of features and conceptual information located in incorrect classes are recognized to improve the results. At this step, it is important to choose the weight of parameters. Relations of segmentation parameters are explained in the Eqs. (2) to (6).

$$f = w_{color}.\Delta h_{color} + w_{shape}.\Delta h_{shape} \tag{2}$$

$$\Delta h_{shape} = w_{compt}.\Delta h_{compt} + w_{smooth}.\Delta h_{smoth} \tag{3}$$

$$\Delta h_{color} = \sum_c w_c(n_{merge}\sigma_{c,merge} - (n_{obj-1}\sigma_{c,obj-1} + n_{obj-2}\sigma_{obj-2})) \tag{4}$$

$$\Delta h_{compact} = n_{merge}.\frac{l_{merge}}{\sqrt{n_{merge}}} - (n_{obj}.\frac{l_{obj-1}}{\sqrt{n_{obj-1}}} + n_{obj-2}.\frac{l_{obj-2}}{\sqrt{n_{obj-2}}}) \tag{5}$$

$$w_{color} + w_{shape} = 1 \qquad w_{compt} + w_{smooth} = 1 \tag{6}$$

In the relations above, Δh_{color} and Δh_{shape} refer to spectral and shape heterogeneity in image objects, respectively. Δh_{compt} as density-derived heterogeneity and Δh_{smooth} as smoothness-derived heterogeneity must be determined to estimate shape heterogeneity. W_{compt}, W_{color}, W_{shape} and W_{smooth} refer to weight and impact of each parameter. They range from 0 to 1. Estimation of the parameters thus leads to heterogeneity parameter of f defined for each image object at each level. Given that diversity of spectral heterogeneity

within some detectable classes of the image can cause disturbance in classification of other objects, scale parameter should be determined for each of them at separated levels. Some samples are chosen from each class and the resolution is analyzed on an appropriate scale to assess spread of classes of features in accordance with scale changes. According to graphs of the Figure 4, the scale of 40 for class of water bodies, the scale of 30 for class of roads and buildings, the scale of 20 for class of vegetation and shadow and the scale

of 10 for classes of paths and other objects are defined. The most appropriate scale of each class of objects is the highest value better adapted to the real object with the least number of segmented objects. Therefore, each object has the best conditions to be extracted and segmented only on a segmentation scale regarding its real dimensions. As the number of references decreases for recognition and classification, computing power can be applied to increase feature space in classification step. Given the noise in satellite images of complex urban areas, a decrease in impact of noise on the results of land cover classification in such areas is another advantage of choosing the biggest scale. It is difficult to choose a scale for classes with a high diversity in spectral properties and intensive spectral and shape heterogeneities. According to graphs of the figure, scale

change includes horizontal areas as well as ascending parts. At this step, there is no significant change in area of image object while increasing segmentation scale that indicates sustainability of resulted objects within the range of scales. So the optimal scale is located on a horizontal part. Segmentation parameters are defined based on local conditions. Area of given classes including roads and buildings are analyzed to determine behavior of the scale. Selection of classes is in accordance with diversity and heterogeneity in spectral behavior of urban areas and their impacts on classification of other features. Five samples of different spectral heterogeneity and dimensions are chosen from each class and their areas are described at segmentation levels. Each class approximately occupies 75% of land cover of the area on selected scale.
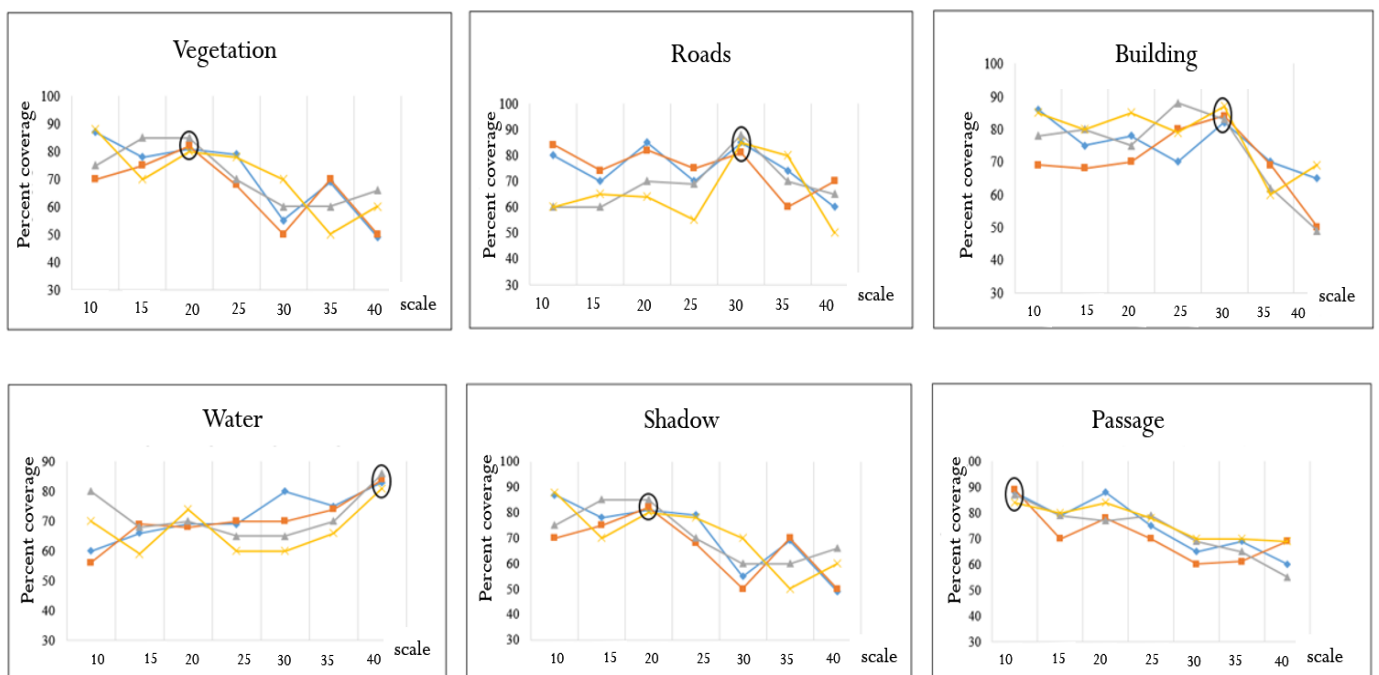

Figure 4. Comparison of scale rate for objects classes

3.2. Proposing a Hierarchical Model

At this step, a hierarchical model is proposed based on multi-resolution segmentation. The model improves classification of features and reduces noises between classes in the urban area. The model is aimed at regulating classification of the features.

3.2.1. Fuzzy Rule-Based Classification

Fuzzy rule-based conceptual method is essentially planned to decline spectral noises of pictorial objects. Proposing a hierarchical model based on given characteristics reduces noises between classes. In conceptual rule-based classification, distinctive characteristics of classes are chosen and their value is determined for various classes. The features are thus recognized through proposed hierarchical

model and specifying thresholds. In complex urban areas, radiometric spectral features lower the efficiency of common classification methods; so it is necessary to utilize whole characteristics of image objects. Features making classes distinguishable should be identified. When a proper feature is selected, its variation range is specified and different classes are recognized based on the hierarchical model. Geometrical, spectral and conceptual features are explained in detail as in the following. It must be noted that the proper feature must make classes distinguishable from each other and does not merely define characteristics of each class. At this step, distinctive attributes of each class of features are initially selected. The feature environment includes three types of geometrical, spectral and conceptual features.

3.2.1.1. Classification of Water Body

Threshold-based detection of water bodies depends on pixels. The most important feature of water is its energy absorption in near-infrared wavelengths. Various indices have been introduced for automatic detection of water types among which normalized difference water index (NDWI) is of great importance (Eq. 6). According to the researches mentioned in the introduction section, infrared spectral range is suitable for detection of free waters but near-infrared range cannot be lonely appropriate for water detection due to turbidity of water or existing plants. So indices are generated by combination of near-infrared band with the other. In fact, a small proportion of radiated energy on water surface is reflected or transmitted. If water body is too deep, energy is absorbed before striking the floor and muddy water has more ability to transmit and reflect it. A considerable proportion of solar radiation striking the water body is absorbed in depth up to 2 m. Water has a low reflectance within near-infrared band but it is not merely efficient to detect water surfaces and the feature cannot be employed to recognize other bodies. In this study, another index known as EWI[1] is applied to detect water bodies [Eq. (8)]. Reflectance of water is maximized in green band and minimized in near-infrared range. Moreover, high reflectance in near-infrared range is associated with soil and vegetation. The index can thus detect all water bodies properly in closed regions. So at this step, water body is detected in a more certain way by another index introduced.

$$NDWI = \frac{Green-NIR1}{Green+NIR1} \quad (7)$$

$$EWI = \frac{Green-NIR1}{(Green+NIR1)\times(NDVI+NIR1)} \quad (8)$$

3.2.1.2. Detection of Roads

Roads are objects with a smooth surface and low diversity on grey-scale. Road areas have lower density because of their linear shapes. Features of linear objects are employed to classify them; for example, the ratio of length to width has a great value in linear objects. Road areas have a smooth surface with a low diversity on grey-scale, so that its length measurement can be appropriate. Classification of roads is one of challenges in the classification of features. Considering shape features of the class, spectral features are initially described.

Here, spectral features include spectral similarity to adjacent image objects. Main characteristics of roads and descriptions used for detection those characteristics are listed in the Tables 1 and 2.

Table 1. Features defined for roads

Item	Features of roads
1	smooth surfaces with low variation on grayscale
2	linear objects with low geometrical density
3	long linear features

Table 2. Description for features of class of roads

Item	Feature	Formulation	Explanation
1	standard deviation	$\sqrt{\frac{1}{n-1}\sum_{i=1}^{n}(C_{Li}-\overline{C_L})^2}$	linear image objects with a low standard deviation
2	ratio of length to width	$\frac{Length}{Width}$	image objects which have higher ratio of length to width
3	Density	$\frac{Length \times Width}{N}$	image objects which have lower density
4	ratio of twice root of area to perimeter (f_1)	$\frac{2\sqrt{\pi.Area(x)}}{Perimeter(x)}$	image objects which possess lower values
5	ratio of area to square of length (f_2)	$\frac{Area(x)}{[Length(x)]^2}$	image objects which possess lower values

- **Density:** This feature indicates geometrical density of the object and is calculated via multiplying length by width and then dividing the total by number of pixels of the object. The result ranges from 0 to 1. So road areas have lower density due to their linear shape.

- **Standard deviation:** This feature indicates variation in digital number of pixels of the image object [Eq. (8)]. Road objects have smooth surfaces with low diversity on grey-scale and this feature can be utilized to detect them. As standard deviation increases, the image object is more probable to be a road. Eq. (9) presents the associated fuzzy set for Standard deviation.

$$\mu_1(x) = \begin{cases} 1-\frac{x}{T}, & for\ 0 \leq x \leq T \\ 0, & Otherwise \end{cases} \quad (9)$$

[1] Enhanced Water Index

87

3.2.1.3. Detection of Buildings

To detect building objects, it is necessary to produce a feature space capable to distinguish buildings from other features. Descriptors must be created in accordance with geometrical and structural features. One of the main features of buildings in large scale satellite images is their rectangular shapes. This feature can be considered as a characteristic of this class of features. So, fitting into rectangles and ellipses and area of objects are described as main characteristics to detect buildings.

Parameter of fitting into rectangle refers to how an image object suits a rectangle and its similar features and parameter of fitting into ellipse indicates how an image object suits an ellipse (Figure 5). Both parameters range from 0 to 1; 1 means that the object completely fits in the given shape. Geometrically, a building has a compacted form like a polygon. So, approximation of the given feature is based on a polygon or ellipse. Consequently, the fuzzy set best fitted into rectangles and ellipses are obtained via Eqs. (10) and (11).

$$\mu_{Rectangule\ Fit}(x) = \begin{cases} 1 - \dfrac{1-x}{1-T}, & for\ 0 < x - T < 1 - T \\ 0, & otherwise \end{cases} \quad (10)$$

$$\mu_{Elliptic\ Fit}(x) = \begin{cases} 1 - \dfrac{1-x}{1-T_2}, & for\ 0 < x - T < 1 - T \\ 0, & otherwise \end{cases} \quad (11)$$
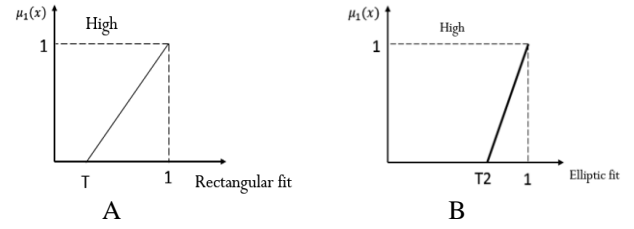

Figure 5. Fuzzy membership functions:
A)   Rectangular fit, B)   Elliptic fit

Building roofs are generally made of materials such as concrete, asphalt, brick, etc. and rarely contain vegetation or water. Road surfaces are somewhat the same as roof covers regarding spectral characteristics. Many buildings and open spaces such as parking lots and paths have a linear form like roads from a geometric point of view. The main class of existing features within an image includes roads, vegetation like trees and grasslands, buildings and open spaces like paths, naked soil, shadows, etc. Spectral features are employed as well as structural characteristics.

- **Area:** a distinctive feature of features with regular geometry like buildings is their area. A specific range is defined for buildings to prevent from classification of all rectangular things like cars. The smallest dimensions defined for a building is 3×4 m and the biggest sizes are considered as 20×25 m. According to resolution of the given image, borders of a building are illustrated within 50 to 2000 pixels, where areas falling in range from 100 to 1500 are more probable (membership degree 1).

- **Average area:** since buildings have particular geometrical properties, features describing geometry of the object are used for as a useful tool for detection according to what is listed in the Table 3.

Table 3. Description for features of class of buildings

Item	Feature	Formulation	Explanation
1	Borders Indicator	$\dfrac{Primeter}{2 \times (Length + width)}$	indicating approximation to a polygon
2	Asymmetry	$1 - \dfrac{Minor\ Axis}{Major\ Axis}$	comparing an object with a regular polygon
3	Concentration	$\dfrac{\sqrt{\sum P_v}}{1 + \sqrt{\sigma_x^2 + \sigma_y^2}}$	describing spatial distribution of pixels of an image object
4	Density	$\dfrac{Length \times Width}{N}$	selecting image objects which have lower geometrical density

The corresponding Fuzzy membership function used for this category is according to Eq. (12) and Figure 6.

$$\mu(x) = min\left\{2 - 2\left(\frac{a\ x|}{c}\right), 1\right\}\ for\ a - \lambda \le$$
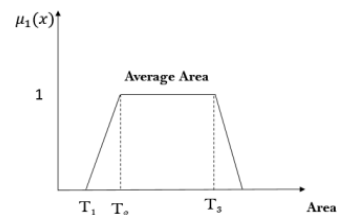$$|a - \lambda| \le a + \lambda;\ \mu(x) = 0 \quad (12)$$

Figure 6. Fuzzy membership functions for area

- **Concentration:** it describes distribution of pixels of the image object by an equation where the numerator is diameter of the rectangular object with $\sum P_v$ pixels and $\sqrt{\sigma_x^2 + \sigma_y^2}$ is diameter of the ellipse fitted into the object. Most of rectangular objects are highly concentrated. Long shapes like shadows have a low concentration. In this study, shadows are employed to detect buildings. Therefore, maximum concentration of shadows is less than 1. Approximation of concentration is based on polygons. The feature indicates distribution of pixels of image objects with the greatest value occurred in square forms. The feature declines as the object become more linear.

- **Adjacent shadows:** square parcels or classes cause reduction of classification accuracy while detecting buildings. Stuff placed on roofs and imperfect segments may also happen during segmentation. According to location of the sun, a building cast a shadow in the opposite direction of the azimuth. Shadows must be observed in a specific length and direction beside buildings. So parameter of shadow can be utilized for better detection. To apply this feature, building height and the azimuth of sun radiation must be considered. Direction of shadows depends on the azimuth of solar direction during imagery process. As illustrated in Figure 7, a shadow can fall in part 1 or 2 according to direction of the building. Direction of shadows can be specified in accordance with geographical location of the object and imagery time.
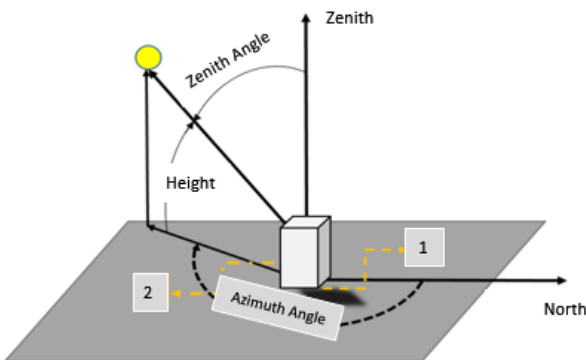

Figure 7. Shadow analysis for building extraction

3.2.1.4. Detection of Shadow Areas

Shadow falls in an image when the light does not directly illuminate whole or some part of an object. The phenomenon accounts for a considerable percentage of VHR images. Logical modelling of shadow is explained as the following:

Shadows are very distinguishable from their surroundings and occupy a small area. By the way, shadows have a high threshold regarding brightness. Shadows are one of the features which may cause incorrect classifications in satellite images. In some cases, shadows are considered as obtrusive objects causing mistakes in classification. So, it is so important to detect and label such features. In addition, shadows represent extruded objects like buildings so that they can be noticed as a feature to detect extruded features. Since shadows are cooler than other areas, *NIR1* band which exists in satellite images derived from WV2 can properly extract such areas.

NIR1 and *NIR2* spectral bands and also blue band are very efficient to detect shadows. HSV[2] colour model is of great importance among colour spaces already introduced because of more adaptation to human eye. *HSV* colour space has three main components which are not completely independent from each other and form a conical coordinate system. At this step, the image is initially converted from RGB space to *HSV* colour model according to the Eqs. (13) to (15).

$$V = \frac{1}{3}(R + G + B) \qquad (13)$$

$$S = 1 - \frac{3}{R+G+B} \qquad (14)$$

$$H = \begin{cases} \theta & if\ B \leq G \\ 360 - \theta & if\ B > G \end{cases} \qquad (15)$$

According to particular features of shadow areas in *HSV* space, the image resulted from different indices for shadow detection and normalization of picture in *HSV* colour model in saturation space is considered as a primary render to recognize shadows.

In this study, module of band math is used in *ENVI* software in order to develop shadow detection index (*SDI*) from various bands if the satellite image. Two types of this index were used in the current research [Eqs. (16) and (17)]. Confusion matrix is also applied to evaluate accuracy of *SDI*. The index has been assessed in different research areas and acceptable results have been achieved.

$$SDI(1) = \frac{Hue}{NIR1} \qquad (16)$$

$$SDI(2) = \frac{Blue - NIR1}{NIR1 + NIR2 + Blue} \qquad (17)$$

---

[2] Hue-Saturation-Value

3.2.1.5. Classification of Vegetation

Detection of vegetation by satellite images is generally carried out by vegetation indices. The indices are resulted from mathematical combination of various digital satellite images which use significant differences in reflectance of vegetation within visible and near-infrared wavelengths and are expressed in terms of simple algebraic equations or linear combinations that convert value of each pixel of various bands into a numerical index and have the highest sensitivity to spectral response of plants. Given high reflectance of vegetation within spectral range of *NIR* band of electromagnetic spectrum, *NIR* ratio is determined for areas with dense vegetation via Eq. (18).

$$NIR\ Ratio = \frac{NIR1}{NIR1+R+G+B} \qquad (18)$$

Red and near-infrared bands play a key role in construction of vegetation indices. Red radiation is absorbed by chlorophyll in plants and infrared radiation is intensively reflected by cellular structures (Eq. 19).

$$NDVI = \frac{NIR1-R}{NIR1+R} \qquad (19)$$

Reflectance differences of these two classes in visible bands and also their differences in absorption and reflection of red and near-infrared bands can be used. In urban regions, grass areas are better irrigated than trees so that they seem fresher. Since class of trees has a high threshold in red and near-infrared bands and class of grass has a low threshold in these three bands, *NDVI* solely is not an appropriate index for detection of these two classes.

3.3. Discussion

To analyze the efficiency of the proposed approach, three blocks of the study region and original image are studied through implementation of fuzzy/non-fuzzy classification methods. The rules applied for detection of classes are listed in Table 4.

Table 4. Rules used to detect classes

| Rule	Condition	Class
rule 1	if value of *EWI* and *NDWI* is high, then	water body
rule 2	if value of feature f_1, f_2, standard deviation and density is low, then	roads
rule 3	if approximation to rectangle, ellipse and circle is high and area is moderate and shadow falls in north west direction, then	buildings
rule 4	if value of *SDI (1)* and *SDI (2)* is high, then	shadows
rule 5	if value of *NDVI* and *NIR* ratio is high, then	vegetation
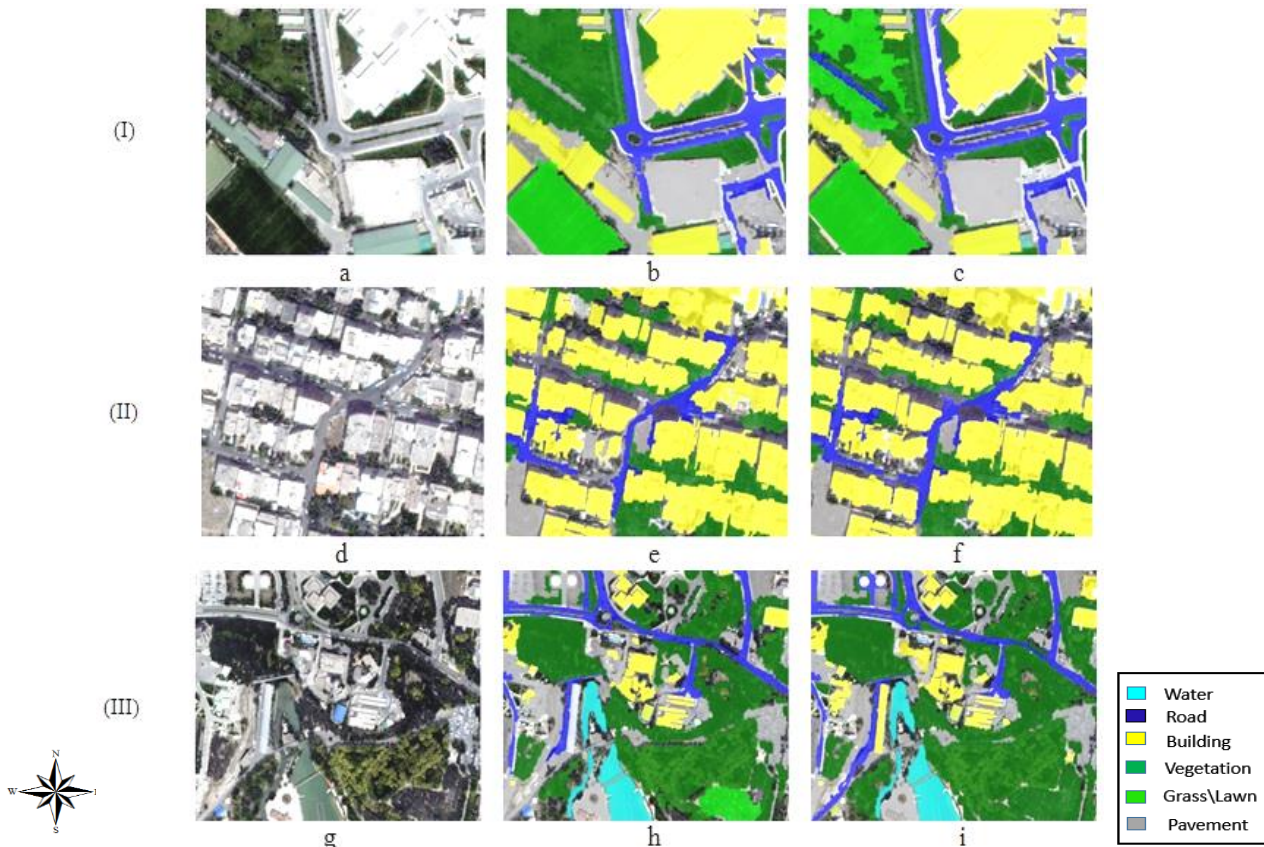
Figure 8. Classification of featured with and without Fuzzy method, (a,d,g) Blocks of the original images, (b,e,h) Blocks of classified images without Fuzzy method, (c,f,i) Block of classified images with Fuzzy method.

90

As the results of rule-based classification indicate in Figure 8, the detection of classes is accomplished appropriately. At this step, training samples are chosen in a proper distribution. Number of training samples is based on class of objects in the Table 5. Google Earth imagery of the region was used to produce ground truth data. Parameters that were used in determination of accuracy of feature classification for each block model are listed in Tables 6 to 7.

Table 5. Training samples

Feature Category	Number of Training Samples
Water	5
Building	20
Road	10
Vegetation	10
Shadow	20

Table 6. Feature classification accuracy parameters {Block (I, II, III), Method 1}

Accuracy Parameters				Category	Block
Overall Accuracy	Kappa Coefficient	User Accuracy	Producer Accuracy		
83 %	0.86	89	87.9	Road	(I)
		94	79	Building	
		1	81	Shadow	
		98	83	Vegetation	
83%	0.81	89	81	Road	(II)
		94	80	Building	
		1	86	Shadow	
		98	84	Vegetation	
81.2 %	0.79	89.2	87.3	Road	(III)
		94	83	Building	
		1	79	Shadow	
		98	84	Vegetation	

Table 7. Feature classification accuracy parameters {Block (I, II, III), Method 2}

Accuracy Parameters				Category	Block
Overall Accuracy	Kappa Coefficient	Producer Accuracy	User Accuracy		
89.7 %	0.9	91	89	Road	(I)
		87.7	94.5	Building	
		92	1	Shadow	
		93	98	Vegetation	
91 %	0.89	89.9	89	Road	(II)
		84	94	Building	
		89	1	Shadow	
		91	98	Vegetation	
89.1 %	0.88	91.9	89	Road	(III)
		87	94	Building	
		89	1	Shadow	
		90	98	Vegetation	

Table 8. Overall accuracy and Kappa coefficient of the presented method and the check project

	Fuzzy Rule-based Method	Regardless of Fuzzy Classification
Overal Accuracy	0.89	0.78
Kappa Coefficient	0.87	0.76

This research is focused on operational aspects and simplicity of implementation. So, fuzzy rule-based classification was used. The results of this technique were compared to Support-Vector Machine and Random Forest methods (Table 8).

4. Permeability of Objects to Radioactive Radiation

Radioactive materials are environmental contaminants resulted from nuclear explosions. Damages from radiation remain for a long time and transmit to later generations and are not limited to specific time and place of the incident. The material contains electromagnetic radiations such as x and γ and nuclear radiations such as x-ray, electrons, protons and neutrons. Radioactive materials are imbalanced isotopes of an element that get balanced by absorbing or losing nucleons

and extra radiation. Radioactive elements may get more sustainable while breaking down. Radioactive materials radiate β, x and γ and they exist in natural and synthetic forms. Some radiations such as x and γ are electromagnetic radiations while the other such as α, β, neutrons and protons are particles moving at very high speeds. Gamma radiation has a great permeability and it can transmit through the air and body layers and cause injuries. It is possible to model emission of radioactive materials and identify its effective factors through study on nuclear disasters which have already happened. Nuclear experts have suggested analytical models to assess pollution rate and permeability of radioactive contaminants.

A wide range of active radionuclides were produced as a result of a nuclear fission. As demonstrated in Table 4, the radionuclides have a greater atomic number than uranium. Cesium 137 nucleoside causes the highest contamination among them. According to the research by experts in International Atomic Energy Agency, EDEM[3] is a developed model to calculate vulnerability of materials based on received dose. The model was suggested after Chernobyl disaster (Anderson, 2003). As illustrated in Figure 9, contamination rate is determined at different levels from 1986 (after disaster) to 2006. Most of damage is associated with features such as soil and vegetation.
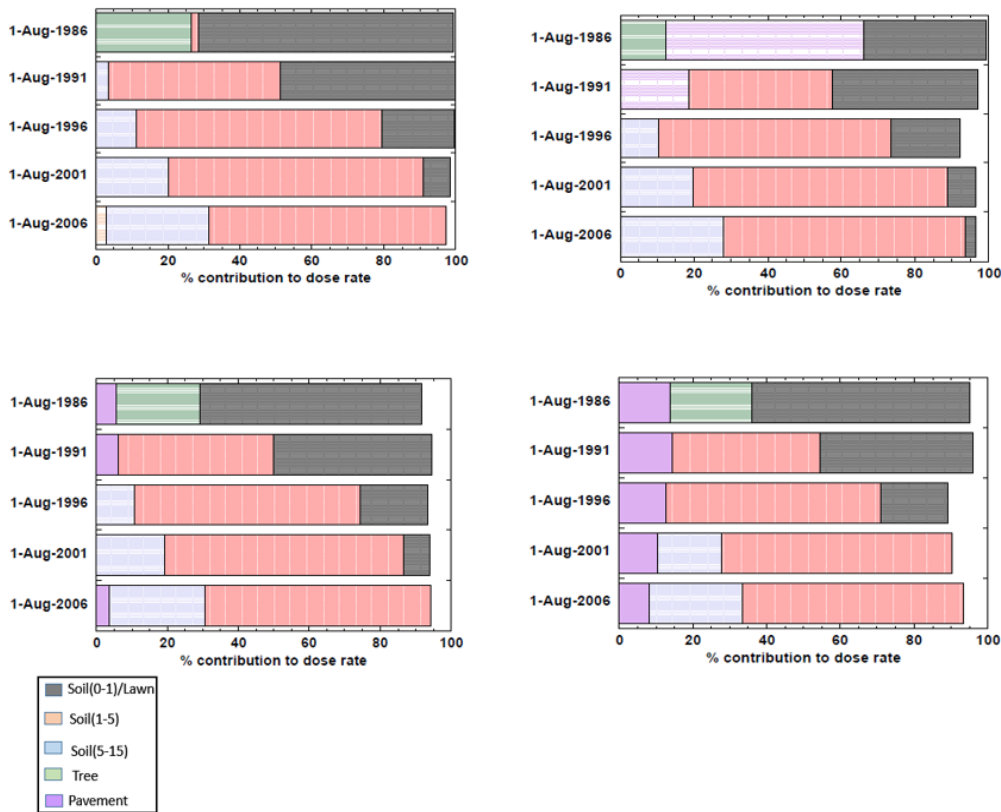

Figure 9. The rate of contamination on the features after the Chernobyl disaster

---

[3] Effective Dose Estimation Module

Each diagram in Figure 9 shows pollution rate after hazard based on measured radioactive contaminations in four different points near the event position. Radioactive radiations are made of radionuclides. According to the reports by nuclear experts, there were different rates of permeability and pollution after disaster. So, as demonstrated in the diagram (1), amount of pollution and rate of permeability depend on material of features.
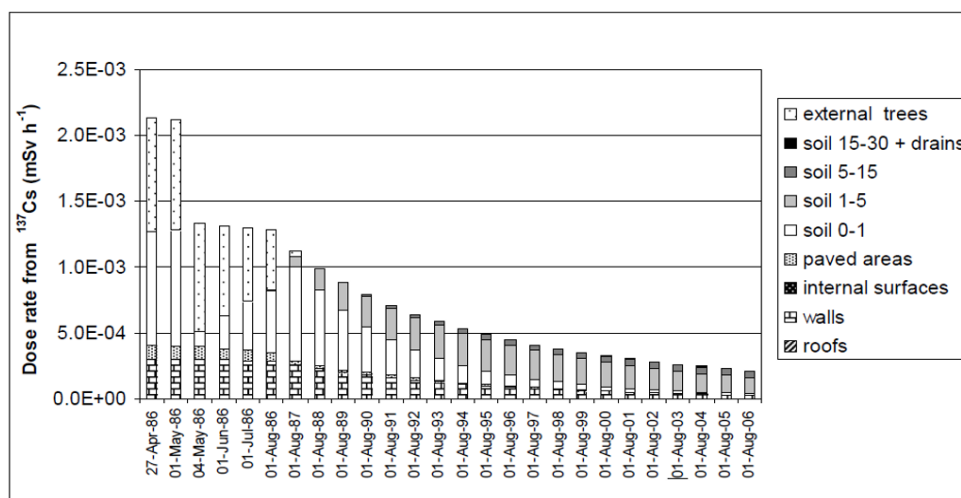

Diagram 1. The different levels of contamination after the nuclear disaster after the Chernobyl nuclear disaster

According to pollution rate of various materials illustrated in the graph below, trees have the most permeability to radiation in first days after Chernobyl disaster. Based on EDEM model and density of radioactive materials after the disaster, features such as vegetation and soils are highly exposed to radiation; such phenomena today occupy limited areas in urban environments. The model is suggested to calculate contamination rate.

5. Risk Analysis of Features

In addition to experiments by more data and other methodologies in this study, the results provided by modeling Chernobyl disaster are matched to other regions and a risk zoning maps are produced using moderate and high resolution images. The proposed model is overlaid on a Landsat image of Tehran. The image is provided by WV2 sensor that is 5 Km far from Atomic Energy Organization in Tehran.

In the current study, medium-resolution Landsat image was applied for macro-zonation that leads to a general description of region zones. Afterwards, high-resolution WorldView image was used for micro-zonation based on the resulted model of Landsat data. This procedure leads to a detailed description of region zones.

Data on distance from residential areas and climatic and topographic parameters collected from websites of NOAA weather service, USGS geological survey, mineral exploration organization of Iran and MapCruzin are processed. According to explanations presented in the previous section about Chernobyl model, hazard zonation map is produced for the region. Given spectral behavior of ingredients of urban features, each material shows a different behavior regarding permeability to radiation. If material used in features is determined by its spectral behavior, its permeability to radiation can be found. So permeability of each object can be determined by specifying its material. At this step, hazard zones are determined through implementation of Chernobyl model and proposed model on a Landsat image of Tehran. Permeability of various features to radioactive contaminants varies with their material. Given the research, pollution of each phenomenon can be identified in the region in case of probable nuclear disaster. As mentioned before, vulnerability of each phenomenon can be modeled in accordance with its material and permeability. It is possible to make decisions based on reports and research by experts in International Atomic Energy Agency regarding environmental and climatic conditions of Chernobyl accident. The risk analysis can be implemented based on the studies in case of assumed disaster. The risk of phenomena is demonstrated in the Figure 9 based on reports and research in the region.

5.1. Vulnerability Modelling

In order for risk assessment to be valid, certain elements must be considered as critical factors. In performing hazard risk assessment of the region of interest, what are likely to be affected by the hazard is of prominent importance to the study. According to the results of measurements performed for each urban feature class and expert opinions, weighting was carried out for determination of features vulnerability level (Table 9).

Table 9. Weighting feature vulnerability level

Feature Class	Vulnerability Weight
Soil	0.70
Vegetation	0.80
Road	0.75
Pavement	0.60
Building	0.50

The vulnerability layer was modelled by weighting and combining the elements using the Single Output Map Algebra function of ArcMap software (Figure 10). The elements were weighted and used to model the vulnerability as follows:

$$VL = (S \times 0.7)+(V \times 0.8)+(R \times 0.4)+(B \times 0.5)+(P \times 0.6) \quad (20)$$

In which

VL: Vulnerability Layer
S: Soil
V: Vegetation
R: Road
B: Building
P: Pavement

Figure 10. Vulnerability layer of the study area

5.2. Hazard Modelling

Since topographic status of the region affects the amount of risk, slope and wind direction layers can also be considered as risk elements. In order to apply wind direction layer in the determination of high-risk zones, it is necessary to establish an information layer in which wind direction is known at each point. Because of the lack of such layer and as it would be illogical to use interpolation for producing wind direction layer, another method is required. Direction of prominent wind is an appropriate parameter to be used (Table 10).

Table 10. Prominent wind angles

Geographic Direction	Prominent Wind Angle
NE	45.48
NW	117.5
SE	110-119

Recorded data at the nearest synoptic station to the event location were acquired from NOAA site. Table 11 shows fuzzy values for prominent wind direction.

Table 11. Fuzzy values for prominent wind angles with respect to geographic directions

Geographic Direction	Fuzzy Value
North	0.2
North-East	0.2
East	1.0
South-East	0.2
South	0.2
South-West	0.6
West	0.4
North-West	0.4

In the absence of data for these hazards, slope and rainfall parameters were used as proxies to model them (Fig. 11). The elements were weighted and used to model the hazard as follows:

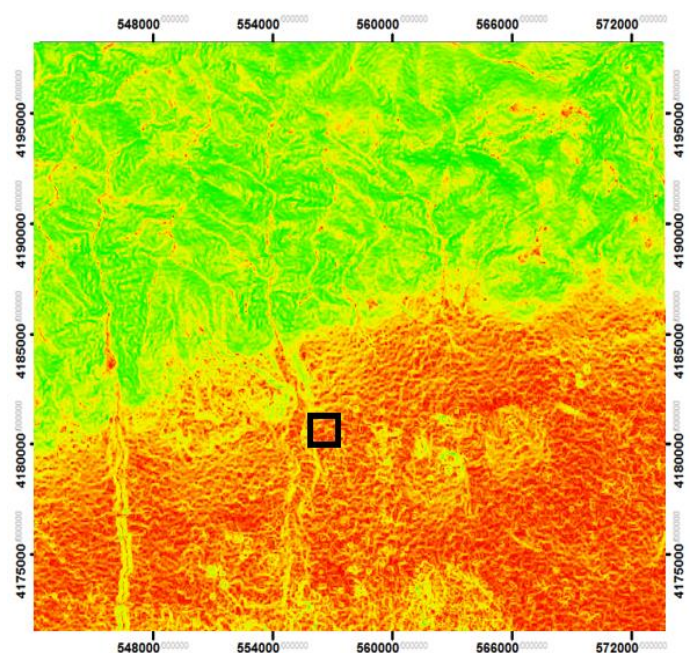$$\text{Hazard Layer} = (\text{Slope} \times 0.6)+(\text{Wind Direction} \times 0.5) \quad (21)$$

Figure 11. Hazard zones of the study area

5.3. Risk Layer

The final risk layer of the study area (Figure 12) was gotten based on level of contamination of radioactive pollution of the region using single Output Map Algebra function of ArcMap software according to Eq. (19). Figure 12 shows pixel values that can be used to represent the several risk areas. These pixel values can be grouped to show a general pattern in the degree of contamination intensity of regions. Thus, with a clearly defined domain of high, moderate to high, medium, moderate to low, risk zones, the technique of density slicing made it possible to reclassify the contamination risk map. This helped to differentiate between areas that experience different intensity of contamination.
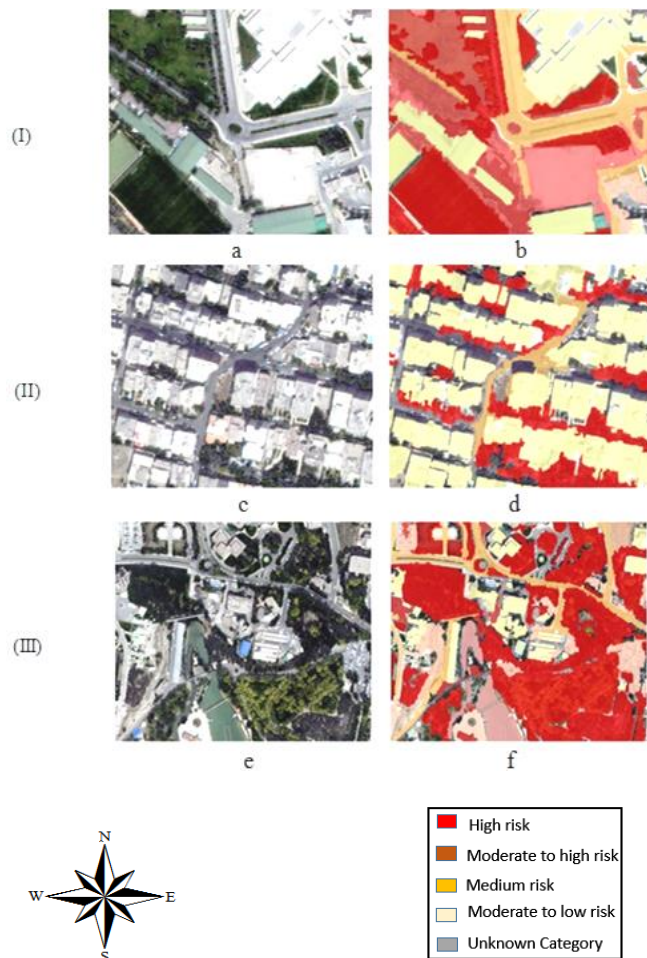

Figure 12. Determination of the amount of risk in the model blocks based on EDEM results. (a,c,e) Original image of blocks, (b,d,f) Determined risk level for identified features of blocks

The vulnerability, hazard and risk maps were all classified into Moderate to Low, Medium, Moderate to High and High risk zones. The multi-risk classification of the zones is displayed on Table 12 to show the areal extent of each zone in the study area.

Table 12. Risk level of each class

Risk Class	Blocks	Area %
High Risk	I	35
	II	18
	III	41
Moderate to High Risk	I	7
	II	8
	III	6
Medium Risk	I	14
	II	11
	III	10
Moderate to Low Risk	I	22
	II	0
	III	10

6. Conclusions

Rule-based methods alone are not efficient and sufficient enough in order to classify complex and developing urban areas. In this study, object-oriented analyses are presented based on multi-scale and hierarchical structures that lead to improved results. Object-oriented classification method is assessed to classify complex urban areas on large-scale images regarding complicated and concentrated urban regions. In this study, fuzzy thresholding of measures is employed to manage uncertainty of segmentation. It is so important to detect land cover of urban areas using large-scale satellite images. Object-oriented methods have eliminated many disadvantages of pixel-oriented methods in image processing. Despite traditional approaches, object-oriented methods benefit from spectral capabilities of images as well as their hidden geospatial aspects. Risk classification of urban features is implemented based on EDEM through the maps generated for each block of the image with the accuracy of 91%. Since vegetation and soil areas have the highest permeability to radioactive pollutants and they reduce density of contaminants in case of disasters, such features are of great importance in urban areas. Based on the analyses performed and zonation maps produced, it is then possible to make all necessary precautions and preparations with emphasis on detected high risk regions, in case of an atomic disaster, to prevent people, national infra-structures and environment from potential threats. It is suggested that for further study, intelligent algorithms, convolution neural network (CNN) or deep learning be applied for enhanced classification.

References

Achanta, R. Shaji, A. Smith, K. Lucchi, A. Fua & P. Süsstrunk, S. (2012). Slic superpixels compared to state-of-the-art superpixel methods. *IEEE Trans. Pattern Anal. Mach. Intell*, Vol. 34, pp. 2274–2282.

Anderson, K. (2003). Radioactive contamination of urban areas. *Journal of Environmental Radioactivity*, Vol. 85, pp. 151–153.

Bardossy, A. & Samaniego, L. (2002). Fuzzy rule-based classification of remotely sensed imagery. *IEEE Transactions on Geoscience and Remote Sensing*, Vol. 40, pp. 362-374.

Benz, U.C. Hofmann, P. Willhauck, G. Lingenfelder & I. Heynen (2004). Multi-resolution, object-oriented fuzzy analysis of remote sensing data for GIS-ready information, *J. Photogramm. Remote Sens*, Vol. 58, pp. 239–258.

Cheng, G. & Han, J. (2016). A survey on object detection in optical remote sensing images. *ISPRS Journal of Photogrammetry & Remote Sensing*, Vol. 117, pp. 11–28.

Douglas, J. (2007). Physical vulnerability modeling in natural hazard risk assessment. *Nat. Hazards Earth Syst.* Sci., Vol. 7, pp. 283–288.

Gabriela, D. (2007). The applicability of fuzzy theory in remote sensing image classification, *Studia Univ.Babes-Bolyai, Informatica,* Vol. LII, No. 1, pp. 89-96.

Gamanya, R., De Maeyer, P. & De Dapper, M. (2009). Object-oriented change detection for the city of Harare, Zimbabwe. *Expert Systems with Applications*, Vol. 36, pp, 571–588.

Ham, J., Chen, M. Crawford, & J. Ghosh (2005). Investigation of the random forest framework for classification of hyperspectral data. *IEEE Trans. Geosci. Remote Sens.*, Vol. 43, pp. 492–501.

Jabari, Sh. & Y. Zhang. (2013). Very high resolution satellite image classification using fuzzy rule-based systems, *Algorithms*, Vol. 6, pp. 762-781.

James, C. R. & Ehrlich, W. (1984). Full-FCM: The fuzzy c-means clustering algorithm. *Computers & Geosciences*, Vol. 10, No. 2-3, pp. 191-203.

Jinmei, L. & Guoyu, W. (2011). A refined quadtree-based automatic classification method for remote sensing image. *International Conference on Computer. Science and Network Technology (ICCSNT)*, pp. 1703–1706.

Jordi, I. (2007). Automatic recognition of man-made objects in high resolution optical remote sensing images by SVM classification of geometric image features. *ISPRS Journal of Photogrammetry & Remote Sensing*, Vol. 62, pp. 236–248.

Kindap, T. (2008). Identifying the trans-boundary transport of air pollutants to the city of Istanbul under specific weather conditions. *Water, Air, and Soil Pollution*, Vol. 189, pp. 279–289.

Liu, D. & Xi, F. (2010). Assessing object‑based classification: advantages and limitations. *Remote Sens. Lett,* Vol. 1, pp. 187–194.

Liu, X., Clarke, K. & Herold, M. (2006). Population density and image texture: A comparison study. *Photogrammetric Engineering& Remote Sensing*, Vol. 72, pp. 187-196.

Lizarazo, I. & Elsner, P. (2009). Fuzzy segmentation for object-based image classification. *Int. J. Remote Sens*, Vol. 30, pp. 1643–1649.

Maurer T. (2013). How to pan-sharpen images using the Gram-Schmidt pan-sharpen method. *International Archives of the Photogrammetry, Remote Sensing and Spatial Information Sciences*. Vol. XL, pp. 239-244.

Ouyang, Z., Zhang, Xie, X. Shen, Q. Guo & Zhao, B. (2011). A comparison of pixel-based and object-oriented approaches to VHR imagery for mapping saltmarsh plants. *Ecol. Inf*, Vol. 6, pp. 136–146.

Pearce, L. (2000). An integrated approach for community hazard, impact, risk and vulnerability analysis: HIRV. *University of British Columbia. Doctoral Dissertation*.

Ramcap, P. (2009). All hazard risk and resilience, prioritizing critical infrastructure by using the RAMCAP plus SM approach. *ASME Innovative Technologies Institute,* ISBN: 9780791802878.

Ravi, C. (2020). Image classification using deep learning and fuzzy systems. *Advances in Intelligent Systems and Computing*, Vol. 941. doi: 10.1007/978-3-030-16660-1.

Réjichi, S., Chaabane, F. & Tupin, F. (2015). Expert knowledge-based method for satellite image time series analysis and interpretation. *IEEE Journal of Selected Topics in Applied Earth Observations and Remote Sensing*, Vol. 8, No. 5, pp. 2138-2150.

Saberi, I. & He, D. (2013). Automatic fuzzy object-based analysis of VHSR images for urban objects extraction. *J. Photogramm. Remote Sens*, Vol. 79, pp. 171–184.

Salehi, B. Zhang, Y. Zhong, M. & Dey, V. (2012). A review of the effectiveness of spatial information used in urban land cover classification of VHR imagery. *Int. J. Geo Inf*, Vol. 8, pp. 35–51.

Sanchez, A. & Azofeifa (2011). Estimation of the distribution of Tabebuia guayacan (Bignoniaceae) using high-resolution remote sensing imagery. *Sensors*, Vol. 11, No. 4, pp. 3831–3851.

Sanchez, C., Hernandez, D. Boyd & G. Foody (2007). One-class classification for mapping a specific land-cover class: SVDD classification of fenland. *IEEE Trans. Geosci. Remote Sens.*, Vol. 45, No. 4, pp. 1061–1073.

Shackelford, A. & Davis, C. H. (2003). A hierarchical fuzzy classification approach for high-resolution multispectral data over urban areas. *IEEE T. Geosci. Remote. Sens*, Vol. 41, pp. 1920–1932.

Shani, A. (2006). Landsat image classification using fuzzy sets rule base theory. *San Jose State University, Washington, USA, Master's Thesis.*

Socolow, R., Andrews, F. & Thomas, V. (1994). Industrial ecology and global change. *Cambridge University Press.*

Steinnocher, K., Weichselbaum J. & Kostl M. (2005). Linking remote sensing and demographic analysis in urbanized areas. *First workshop of the EARSeL SIG on urban remote sensing, Australia.*

Sowmya, B. & SheelaRani. B. (2011). Land cover classification using reformed fuzzy c-means. *sadhana*, Vol. 36, pp. 153-165.

Van Westen, C., Montoya, L., & Boerboom, L. (2002). Multi-hazard risk assessment using GIS in urban areas: A case study for the city of Turrialba, Costa-Rica. *Regional workshop on Best Practice in Disaster Mitigation*, pp. 120–136.

Whiteside, T. G., Boggs, G. S. & Maier, S. W. (2011). Comparing object-based and pixel-based classifications for mapping savannas. *Int. J. Appl. Earth Obs. Geoinf.* Vol. 13, pp. 884–893.

Wilkinson, G. (2005). Results and implications of a study of fifteen years of satellite image classification experiments. *IEEE Trans. Geosci. Remote Sens.*, Vol. 43, No. 3, pp. 433–440.

Zhou, W, Huang G. & Troy A. (2009). Object-based land cover classification of shaded areas in high spatial resolution imagery of urban areas. *Remote Sensing of Environment*, Vol. 113, pp. 1769-1777.